UCRL-94630
PREPRINT

MOLECULAR EFFECTS IN TRITIUM β DECAY. III. ELECTRONIC RESONANCES OF HeT^+ ION AND DEPENDENCE OF NEUTRINO MASS ON ACCURACY OF THEORETICAL MODEL

K. Szalewicz
O. Fackler
B. Jeziorski
W. Kolos
H.J. Monkhorst

This paper was prepared for submittal to
Physical Review A

May 1986

MOLECULAR EFFECTS IN TRITIUM β DECAY. III. ELECTRONIC RESONANCES OF HeT^+ ION AND DEPENDENCE OF NEUTRINO MASS ON ACCURACY OF THEORETICAL MODEL

K. Szalewicz,[a,b] O. Fackler,[c,d] B. Jeziorski,[a,b,e] W. Kołos,[a,b] and H.J. Monkhorst[a]

[a]Quantum Theory Project, Departments of Chemistry and Physics, University of Florida, Gainesville, Florida 32611

[b]Quantum Chemistry Laboratory, Department of Chemistry, University of Warsaw, Pasteura 1, 02093 Warsaw, Poland

[c]Department of Physics, Rockefeller University, New York, N.Y. 10021

[d]Lawrence Livermore National Laboratory, University of California, Livermore, Ca 94550

[e]Department of Applied Mathematics, University of Waterloo, Waterloo, N2L 3G1 Ontario, Canada

ABSTRACT

Several theoretical aspects of the β-decay process in T_2 are discussed. New results of the stabilization method calculations for the resonance states of the daughter HeT^+ ion are presented. The probabilities for this system to be found in various final shake-off states after the T_2 decay have been calculated. The β-decay spectra are generated using probability distributions of various accuracies. It is shown that, if the actual neutrino mass were 30 eV, one would obtain masses of 6 and 25 eV using the bare tritium nucleus and the tritium atom spectra, respectively, for analyzing the data. If the nuclear motion effects were neglected, the obtained mass would be 30 eV but the endpoint energy would be shifted by 1.5 eV. For a 30 eV mass the accuracy of our calculations is much better than necessary: substituting our data by those obtained with a very poor basis set changed the neutrino mass by about 1 eV only. For a 1 eV mass, however, the less accurate calculation would lead to a zero mass. In particular, including the effects of nuclear motion is important to correctly determine a 1 eV mass. The accuracy of resonance states of the daughter ion has practically no influence on the final result. We argue that solid state effects will lead to corrections insignificant with respect to the expected experimental errors.

I. INTRODUCTION

During the past 5 years the problem of the neutrino mass has become one of the most discussed and controversial topics in particle physics, astrophysics and cosmology. This development started with measurements of neutrino oscillations[1] and of the tritium β spectrum[2]. Both experiments have been severely criticized (see Refs. 3 and 4 for reviews). In the former experiment new measurements by several groups[3] disproved Reines' et al.[1] finding. Lubimov's et al. neutrino mass experiment[2] has been repeated twice by the same IETP group.[5,6] In response to criticism, each time the authors changed their method of processing the data, but their value of the neutrino mass remained more or less unchanged. Unfortunately, the IETP group did not process their older data with the improved methods. Therefore, one cannot say whether their new results corroborate the previous ones with a more accurate measurement, and whether the changes in the procedures of processing the data were important.

One of the main objections against Lubimov's et al. experiment was their use of a fairly complicated molecule, tritrated valine: $C_5H_{11}NO_2$, as the radioactive source. It has been pointed out already by Bergkvist[7] that a correct account of the effects of atomic or molecular surroundings in the analysis of experimental data is crucial for determining the neutrino mass. In a series of papers, Kaplan, Smelov and Smutny[8,9] presented some calculations of these effects for valine. However, these authors also acknowledge that their results are very approximate due to the size of the system. In another experiment

by Simpson[10] the final state effects are much less important, however, this experiment suffers of rather poor resolution. Therefore, the most promising experiments now underway are those which use the atomic or molecular tritium sources;[11-13] only for such systems accurate quantum mechanical calculations are feasible.

In the two previous publications of this series, which will be referred to as Part I[14] and Part II,[15] we have presented calculations for the β decay of T_2 molecule. In Part I the discrete electronic states of HeT^+ were treated. In Part II the effects of nuclear motion were taken into account for these states. In the present paper we will report an extension of our previous calculations[16] for the remaining, continuous part of the spectrum and for the resonance states embedded in it. All these calculations produced a complete probability distribution for the final states and enabled us to construct an accurate β spectrum for T_2, which has already been published in a Letter.[17] In the present paper we will discuss in more detail several theoretical aspects connected with this spectrum. We will also show how the final value of the neutrino mass depends on the probability distribution used to construct the model theoretical β spectrum. This will be done by fitting spectra of various accuracies to a set of quasi-experimental points generated from our most accurate theoretical spectrum by a Monte Carlo method.

II. THEORY

The neutrino mass extracted from a β-decay experiment will critically depend on the theoretical model used. There are several features of the model - connected with the experimental situation and with the level of theoretical knowledge of the parent and daughter system - the interplay of which can lead to erratic final values. Later we will discuss the results of some numerical experiments examining this problem. Since we did not find a satisfactory theoretical formulation in the literature and since we want to clearly specify all approximations, we will start with a presentation of the theoretical background of the process.

An expression for the β-decay spectrum can be derived from the Fermi theory.[18,19] We will present a nonrelativistic derivation except for using the relativistic relation between the momentum and energy for the β electron and antineutrino. We consider the β-decay of an isolated T_2 molecule, which can be trivially generalized to any molecular case. The products of a T_2 β decay are

$$T_2 \longrightarrow (HeT^+)_n + e^- + \bar{\nu} \qquad (1)$$

where $(HeT^+)_n$ means that the HeT^+ ion is in its nth quantum state Ψ_n^f. We also assume that T_2 was in its ground state Ψ_1^i and that the β electron and antineutrino have momenta $\vec{k}_e$ and $\vec{k}_{\bar{\nu}}$, respectively. The momentum of the HeT^+ ion (the recoil momentum) will then be $\vec{k} = -(\vec{k}_e + \vec{k}_{\bar{\nu}})$.

According to the Fermi theory the decay probability density per unit time for the reaction (1) is given by the familiar golden rule expression[19]

$$R_{i\to f} = \frac{2\pi}{\hbar} |\langle \Phi^f | \hat{H}_\beta | \Phi^i \rangle|^2 \, \delta(E_i - E_f) \tag{2}$$

where Φ^f and Φ^i denote the final and initial quantum states and $\hat{H}_\beta$ is the weak interaction operator responsible for the decay. The operator $\hat{H}_\beta$ can be written in the form[19]

$$\hat{H}_\beta = g \int \hat{\Psi}_p^+(\vec{x}) \, \hat{\Psi}_n(\vec{x}) \, \hat{\Psi}_e^+(\vec{x}) \, \hat{\Psi}_{\bar{\nu}}^+(\vec{x}) \, d\vec{x} + \text{h.c.} \tag{3}$$

where g is the Fermi constant describing the strength of the weak interaction and "h.c." denotes the hermitean conjugate. The field operators $\hat{\Psi}_a^+(\vec{x})$ and $\hat{\Psi}_a(\vec{x})$ create and destroy a particle a at the point $\vec{x}$, respectively. The subscripts p, n, e and $\bar{\nu}$ refer to the proton, neutron, electron, and antineutrino, respectively. The creation operator $\hat{\Psi}^+$ is the hermitean conjugate of the annihilation operator $\hat{\Psi}$. The latter operator acting on a wave function which depends on coordinates of N particles of a given kind produces the following result

$$\hat{\Psi}(\vec{x}) \, \Phi(\ldots, \vec{r}_1, \vec{r}_2, \ldots, \vec{r}_N) = \sqrt{N} \, \Phi(\ldots, \vec{x}, \vec{r}_2, \ldots, \vec{r}_N) \tag{4}$$

where the additional points indicate that the function Φ may depend on coordinates of other kinds of particles. We may write the matrix element in Eq. (2) as

$$T_{if} = \langle \Phi^f | \hat{H}_\beta | \Phi^i \rangle = g \int \langle \hat{\Psi}_p(\vec{x}) \, \hat{\Psi}_e(\vec{x}) \, \hat{\Psi}_{\bar{\nu}}(\vec{x}) \, \Phi^f | \hat{\Psi}_n(\vec{x}) \, \Phi^i \rangle \, d\vec{x} \tag{5}$$

Now we have to specify Φ^i and Φ^f. The former wave function can be written as the product of the wave function describing the internal states of the tritium nucleus and the ground state wave function of the tritium molecule

$$\Phi^i = \chi^i_{nucl} \Psi^i_{T_2}(\vec{R}_{T1}, \vec{R}_{T2}, \vec{R}_{e2}, \vec{R}_{e3}) \tag{6}$$

The variables $\vec{R}_{Ti}$ and $\vec{R}_{ei}$ denote positions of the ith tritium nucleus and of the ith electron, respectively, in the laboratory frame (LF) system. We assume that the T1 nucleus decays and we consider the internal structure of this nucleus, whereas the other nucleus will be treated as a point charge. Therefore, $\vec{R}_{T1}$ denotes the center of mass (CM) of the T1 nucleus. Similarly, the final wave function Φ^f will be assumed in the form of a product of the wave function describing the internal states of the ^{3}He nucleus, the free antineutrino wave, and the wave function for the molecular system HeT of two nuclei and three electrons

$$\Phi^f = \Omega^{-1/2} \chi^f_{nucl} e^{i\vec{k}_{\bar{\nu}} \cdot \vec{R}_{\bar{\nu}}} \Psi^f_{HeT}(\vec{R}_{He}, \vec{R}_T, \vec{R}_{e1}, \vec{R}_{e2}, \vec{R}_{e3}) \tag{7}$$

where Ω is the volume in which the plane wave is normalized. The nuclear wave functions depend on relative coordinates only. Eqs. (6) and (7) introduce the obvious approximation of the independence of the internal nuclear and molecular motions. The action of the annihilation operators in Eq. (5) can be easily calculated

$$\hat{\Psi}_n(\vec{x})\ \Phi^i = (\hat{\Psi}_n(\vec{x}) \chi^i_{nucl})\ \Psi^i_{T_2}(\vec{R}_{T1}, \vec{R}_{T2}, \vec{R}_{e2}, \vec{R}_{e3}) \tag{8}$$

$$\hat{\Psi}_p(\vec{x})\ \hat{\Psi}_e(\vec{x})\ \hat{\Psi}_{\bar{\nu}}(\vec{x})\ \Phi^f = \Omega^{-1/2} (\hat{\Psi}_p(\vec{x}) \chi^f_{nucl}) e^{i\vec{k}_{\bar{\nu}} \cdot \vec{x}} \sqrt{3}\ \Psi^f_{HeT}(\vec{R}_{He}, \vec{R}_T, \vec{x}, \vec{R}_{e2}, \vec{R}_{e3}) \tag{9}$$

The vectors $\vec{R}_{T1}$ and $\vec{R}_{He}$ are now dependent on $\vec{x}$

$$\vec{R}_{T1} = \frac{M_p \vec{R}_p + M_n \vec{R}_n + M_n \vec{x}}{M_p + 2M_n}$$

$$\vec{R}_{He} = \frac{M_p \vec{R}_p + M_n \vec{R}_n + M_p \vec{x}}{M_n + 2M_p}$$

where $\vec{R}_p$, $\vec{R}_n$, M_p, and M_n are proton and neutron coordinates and masses, respectively. Substituting Eqs. (8) and (9) into Eq. (5) we may factorize the integration over $\vec{R}_p$ and $\vec{R}_n$ if we assume that in the very small region around $\vec{x}$ where the nuclear wave functions are localized the molecular and the antineutrino wave functions are constant, equal to their values at $\vec{x}$. After these manipulations Eq. (5) becomes

$$T_{if} = g\sqrt{3}\Omega^{-1/2} M_{nucl} \int \psi^{f*}_{HeT}(\vec{x}, \vec{R}_T, \vec{x}, \vec{R}_{e2}, \vec{R}_{e3})\, e^{-i\vec{k}_{\bar{\nu}}\cdot\vec{x}} \times \psi^{i}_{T_2}(\vec{x}, \vec{R}_T, \vec{R}_{e2}, \vec{R}_{e3})\, d\vec{x}\, d\vec{R}_T d\vec{R}_{e2} d\vec{R}_{e3} \qquad (10)$$

where

$$M_{nucl} = \langle \chi^{f}_{nucl} | \hat{\psi}^{+}_{p}(\vec{x}_0) \hat{\psi}_{n}(\vec{x}_0) \chi^{i}_{nucl} \rangle \qquad (11)$$

$\vec{x}_0$ is an arbitrary value of $\vec{x}$, and $\vec{R}_T \equiv \vec{R}_{T2}$. The nuclear matrix element M_{nucl} is independent of $\vec{x}$ since the nuclear wave functions depend only on the relative coordinates. In the β decay M_{nucl} is constant and therefore we do not need to consider it any further. The expression (10) is practically equivalent to the expression (5) since the only assumption so far (independence of the internal nuclear and molecular motions and the high localization of the nuclear wave functions compared to those for the molecule) are very well satisfied.

To further simplify Eq. (10) we could assume the following factorized form for the HeT wave function

$$\psi^{f}_{HeT}(\vec{R}_{He}, \vec{R}_T, \vec{R}_{e1}, \vec{R}_{e2}, \vec{R}_{e3}) \sim \qquad (12)$$

$$\frac{1}{\sqrt{3}}\, \Omega^{-1}(1 - P^{el}_{12} - P^{el}_{13})\, e^{i\vec{k}_e\cdot\vec{R}_{e1}}\, e^{i\vec{k}\cdot\vec{R}_{CM}}\, \psi^{f}_{n}(\vec{R}, \vec{r}_{e2}, \vec{r}_{e3})$$

where P_{ij}^{el} permutes electrons i and j. The first factor in Eq.(12) describes the β electron as a plane wave. The remaining factors represent the CM motion for the HeT^+ ion and the wave function for the nth internal state of this ion. The relative and the CM coordinates are defined as follows

$$\vec{R} = \vec{R}_T - \vec{R}_{He} \tag{13}$$

$$\vec{r}_{ei} = \vec{R}_{ei} - \vec{R}_{He}\ , \quad i = 1, 2 \tag{14}$$

$$\vec{R}_{CM} = \frac{M_{He}\vec{R}_{He} + M_T\vec{R}_T + m_e(\vec{R}_{e1} + \vec{R}_{e2})}{M_{He} + M_T + 2m_e} \tag{15}$$

where M_{He} and M_T are the masses of He and T nuclei, respectively. We may easily improve upon Eq. (12) by using, instead of the plane wave

$$e^{i\vec{k}_e\cdot\vec{R}_{e1}} = e^{i\vec{k}_e\cdot\vec{r}_{e1}}\, e^{i\vec{k}_e\cdot\vec{R}_{He}} \tag{16}$$

the plane wave deformed by the charge at $\vec{R}_{He}$ which accounts for the interaction of the β electron with the (screened) Coulomb field of He^{++}. This substitution leads to the following form of the HeT wave function

$$\Psi_{HeT}^f = \frac{1}{\sqrt{3}}\,\Omega^{-1}(1 - P_{12}^{el} - P_{13}^{el})\,\psi_{k_e}^C(\vec{r}_{e1})\, e^{i\vec{k}_e\cdot\vec{R}_{He}}\, e^{i\vec{k}\cdot\vec{R}_{CM}}\Psi_n^f(\vec{R}, \vec{r}_{e2}, \vec{r}_{e3}) \tag{17}$$

The Coulomb function $\psi_{k_e}^C(\vec{r})$ can be expressed in a standard way[20] through the confluent hypergeometric function F(a|b|x)

$$\psi_{k_e}^C(\vec{r}) = e^{\pi\eta/2}\,\Gamma(1 - i\eta)\, e^{i\vec{k}_e\cdot\vec{r}}\, F(i\eta|1|i(k_e r - \vec{k}_e\cdot\vec{r})) \tag{18}$$

where

$$\eta = Zm_e e^2/\hbar^2 k_e \tag{19}$$

Γ is the standard gamma function, m_e is the electron mass, $k_e = |\vec{k}_e|$, $r = |\vec{r}|$, and Z is the effective charge of the daughter nucleus. Since in Eq. (10) $\vec{R}_{e1} = \vec{R}_{He} = \vec{x}$, we only need $\psi^S_{k_e}(0)$. The square of the modulus of this function at zero

$$|\psi^S_{k_e}(0)|^2 \equiv F(Z, k_e) = e^{\pi\eta}|\Gamma(1 - i\eta)|^2 = 2\pi\eta/[1 - \exp(-2\pi\eta)] \qquad (20)$$

is known as the Fermi function.

Use of Eq. (17) introduces the first nonnegligible approximations. In this way we neglect: (i) interaction of the β electron with the inactive tritium nucleus (ii) actual screening of the active nucleus and the final states dependence of this screening, and (iii) correlation of the β electron in its continuum orbital with the slow bound-state molecular electrons. The effects (i) - (ii) should be small if $\vec{k}_e$ is large, i.e. if $1/k_e$ is much smaller than the distance between the nuclei and the average distance between the electrons and the He nucleus. At the endpoint energy of 18.6 keV we have $1/k_e = 0.027\ a_0$ and this condition is well satisfied.

The effects (ii) and (iii) were considered by Williams and Koonin[21] who calculated the first-order correction for the interaction between the slow and fast electrons in the case of atomic tritium. This correction was found to change the $|T_{if}|^2$ value by only 0.17% for the two lowest atomic states. Williams and Koonin do not separate the effects (ii) and (iii). It is possible, however, that almost the same result could be obtained by a a simpler treatment including only the effect (ii). For molecular tritium decays these effects should be of similar magnitude as for the atomic case.

Assuming for simplicity that the initial system was at rest and, consistently with experiments, that the T_2 molecule was in its ground state we may write the initial molecular wave function as

$$\Psi^i_{T_2} = \Omega^{-1/2}\Psi^i_1(\vec{R}, \vec{r}_{e2}, \vec{r}_{e3}) \tag{21}$$

Substituting in Eq. (10) the wave functions by the forms given by Eqs. (17) and (21), dropping exchange terms which are known to be negligible,[21] changing the integration variables to those given by Eqs. (13) - (15), and integrating over the CM coordinates we obtain

$$T_{if} = \tag{22}$$
$$= g\Omega^{-1}M_{nucl}e^{\pi\eta/2}\Gamma(1 - i\eta)\int\Psi^{f*}_n(\vec{R}, \vec{r}_1, \vec{r}_2)e^{-i\vec{k}\cdot\vec{r}_c}\Psi^i_1(\vec{R}, \vec{r}_1, \vec{r}_2)\, d\vec{R}\, d\vec{r}_1 d\vec{r}_2$$

where $\vec{r}_c = (M_T\vec{R} + m_e\vec{r}_1 + m_e\vec{r}_2)/(M_{He} + M_T + 2m_e)$, $\vec{r}_1 \equiv \vec{r}_{e2}$, and $\vec{r}_2 \equiv \vec{r}_{e3}$. Neglecting small terms of the order $[m_e k/(M_{He} + M_T + 2m_e)]^2$ we finally obtain the well known[22,23] expression for R_{if}

$$R_{if} = \frac{2\pi g^2}{\hbar\Omega^2}|M_{nucl}|^2 F(Z, k_e)\, P_n(\vec{q})\, \delta(E_i - E_f) \tag{23}$$

The quantity

$$P_n(\vec{q}) = |\langle\Psi^f_n(\vec{R}, \vec{r}_1, \vec{r}_2)|e^{i\vec{q}\cdot\vec{R}}\Psi^i_1(\vec{R}, \vec{r}_1, \vec{r}_2)\rangle|^2 \tag{24}$$

where

$$\vec{q} = -\frac{M_T}{M_{He} + M_T + 2m_e}\vec{k} \tag{25}$$

can be interpreted as the probability density of finding the daughter system in the final state for a given value of the recoil momentum $\vec{k}$.

It was shown in Part II that the dependence of $P_n(\vec{q})$ on the direction of $\vec{q}$ is eliminated after introduction of the adiabatic approximation for Ψ_1^i and Ψ_n^f, application of the standard partial wave expansion for $\exp(i\vec{q}\cdot\vec{r})$, and summing Eq. (23) over the degenerate final states. Using for simplicity the same letters for the summed quantities we may write Eq. (23) as

$$R_{if} = \frac{2\pi g^2}{\hbar\Omega^2} |M_{nucl}|^2 F(Z, k_e)\, P_n(q)\, \delta(E_i - E_f) \tag{26}$$

where $q = |\vec{q}|$.

To obtain the β spectrum for the nth channel (i.e. the dependence of the decay probability density per unit time on the modulus of the β electron momentum k_e) we have to sum Eq. (26) over $\vec{k}_{\bar{\nu}}$ and over the directions of $\vec{k}_e$. Since the plane waves have been normalized in Ω, the factor $\Omega^2/(2\pi)^6$ has to be included when changing summation to integration.[19] If we neglect the dependence of $P_n(q)$ on $\vec{k}_{\bar{\nu}}$ (a good approximation close to the endpoint), the integration concerns only the δ function. The argument of this function can be written as

$$E_i - E_f = M_i c^2 - M_f c^2 - \sqrt{p_{\bar{\nu}}^2 c^2 + m_{\bar{\nu}}^2 c^4} - \sqrt{p_e^2 c^2 + m_e^2 c^4} - E_R - \Delta E_{n1} \tag{27}$$

where $p_x = \hbar k_x$, M_i and M_f are the masses of the initial and final nuclei, respectively, E_R is the recoil energy, and $\Delta E_{n1} = E_n^f - E_1^i$ is the difference of molecular energies corresponding to the functions Ψ_n^f and Ψ_1^i. Performing the integration gives

$$\int R_{if} d\vec{k}_{\bar{\nu}}\, d\Omega_e = \frac{g^2}{2\pi^3\hbar^4 c^3} |M_{nucl}|^2 F(Z, k_e)\, P_n(q) \times \tag{28}$$
$$\times (E_{max} - \varepsilon_n - E_e) [(E_{max} - \varepsilon_n - E_e)^2 - m_{\bar{\nu}}^2 c^4]^{1/2}$$

where Ω_e denotes angles of $\vec{k}_e$, E_e is the total energy of the β electron (including the rest energy), $E_{max} = M_i c^2 - M_f c^2 - E_R - \Delta E_{11}$ is the endpoint energy of the β spectrum for $n = 1$ and $m_\nu = 0$, and $\varepsilon_n = E_n^f - E_1^f$. Multiplying Eq. (28) with $p_e^2\, dp_e$ we obtain the probability of the decay into channel n with electron momentum between p_e and $p_e + dp_e$. This quantity is proportional to the number $dN_n(p_e)$ of β electrons in this momentum range emitted per unit time. Denoting the proportionality constant by A′ we may write

$$dN_n(p_e) = \tag{29}$$
$$= A'F(Z, k_e)\, P_n(q)\, p_e^2 (E_{max} - \varepsilon_n - E_e)\, [(E_{max} - \varepsilon_n - E_e)^2 - m_\nu^2 c^4]^{1/2} dp_e$$

To obtain the total β spectrum Eq. (29) has to be summed/integrated over all the final states. Omitting from now on the subscript "e" we may write the final expression for the β spectrum

$$dN(p) = \tag{30}$$
$$= A'F(Z, k_e)\, p^2 \sum\!\!\!\!\!\!\int_n P_n(q)\, (E_{max} - \varepsilon_n - E)\, [(E_{max} - \varepsilon_n - E)^2 - m_\nu^2 c^4]^{1/2} \times dp$$

Because of the relativistic relation between the momentum and energy $c^2 p\, dp = E\, dE$ and we may write

$$\bar{I}(E) = d\bar{N}(E)/dE = A\, F(Z, k_e)\, p\, E \times$$
$$\times \sum\!\!\!\!\!\!\int P_n(q)\, (E_{max} - \varepsilon_n - E)\, [(E_{max} - \varepsilon_n - E)^2 - m_\nu^2 c^4]^{1/2} \tag{31}$$

where $\bar{N}(E) = N((p^2c^2 + m^2c^4)^{1/2})$ and $A = A'/c^2$. It will also be convenient to consider the spectrum as a function of $E_\beta = E - mc^2$ [$p = (E_\beta^2/c^2 + 2mE_\beta)^{1/2}$]

$$I(E_\beta) = A\, F(Z, k_e) \times \qquad (32)$$

$$\times\, p\,(E_\beta + mc^2) \sum\!\!\!\!\!\!\int P_n(q)\,(W_0 - \varepsilon_n - E_\beta)[(W_0 - \varepsilon_n - E_\beta)^2 - m_{\bar{\nu}}^2 c^4]^{1/2}$$

where $W_0 = E_{max} - mc^2$ and $I(E_\beta) = \tilde{I}(E_\beta + mc^2)$. For each branch of the spectrum the allowed values of E_β are such that $W_0 - \varepsilon_n - E_\beta \geq m_{\bar{\nu}} c^2$. Therefore W_0 is the maximum value of E_β for $n = 1$ and $m_\nu = 0$; for $m_\nu \neq 0$ the endpoint of the spectrum is shifted by $-m_{\bar{\nu}} c^2$.

Instead of the β spectrum it is convenient to present the so called Kurie plot,[24] i.e.

$$\sqrt{\frac{I(E_\beta)}{p\,(E_\beta + mc^2)\,F(Z,k_e)}} =$$

$$= \left(\sum\!\!\!\!\!\!\int P_n(q)\,(W_0 - \varepsilon_n - E_\beta)[(W_0 - \varepsilon_n - E_\beta)^2 - m_{\bar{\nu}}^2 c^4]^{1/2}\right)^{\frac{1}{2}}$$

III. CONTINUOUS SPECTRUM OF HeT^+ ION

A. STABILIZATION GRAPHS

In our preliminary work[16] it has been shown that the energies of the electronic resonance states of HeT^+ can be computed reliably using the stabilization method[25] and a basis set of explicitly correlated functions

$$\phi(\vec{r}_1, \vec{r}_2) = \xi_1^{r_i} \xi_2^{\bar{r}_i} \eta_1^{s_i} \eta_2^{\bar{s}_i} \rho^{\mu_i} \exp(-\alpha_1 \xi_1 - \alpha_2 \xi_2 - \beta_1 \eta_1 - \beta_2 \eta_2) \qquad (33)$$

where ξ and η denote the elliptic coordinates, $\rho = 2r_{12}/R$, $R=|\vec{R}|$, $r_{12} = |\vec{r}_1 - \vec{r}_2|$, α_1, α_2, β_1, and β_2 are nonlinear variational parameters and r_i, $\bar{r}_i$, s_i, $\bar{s}_i$, and μ_i are integers. These computations have been extended, using the same 200-term expansion of the wave function and searching for the optimum values of the exponents. This resulted in improved stabilities of the resonance energies, especially for intermediate values of R. As an example we present in Fig. 1 a stabilization graph computed for R = 1.4 bohr. The energies are shown as functions of an overall scaling parameter, s, applied to the exponents in the function (33). When compared with Fig. 3 in Ref. 16, the improvement is clearly seen, especially for the higher resonance states. The results also indicate that to get stable energies for various resonance states different sets of exponents must be used. This is, of course, not surprising for states corresponding to different electronic configurations.

Determination of the energies of the 5 lowest resonance states of HeT^+ did not present any essential difficulties over a wide range of internuclear distances. For higher states, however, problems have been encountered. It was not uncommon that a resonance state, clearly seen on a stabilization graph computed with one set of nonlinear parameters, disappeared if other initial values of the exponents were used. Sometimes an apparently sharp resonance state was obtained for a certain internuclear distance but it was difficult, or impossible, to find this state at an adjacent internuclear distance. For higher energies such problems are quite natural, since the borderline between a resonance and a scattering state becomes diffuse. In Table I we list the computed energies of the resonance states. For the 5 lowest states the results are complete. For the higher ones we list only those energies that seemed to be highly reliable. To obtain the energies, the point of the best stability was estimated from the graph and the value of the energy at this point was linearly interpolated from two closest calculated points. It is difficult to assess the accuracy of the results. The error can certainly affect the last figure quoted.

There are three possible dissociation channels of HeT^+: $He^+ + T$, $He + T^+$, and $He^{++} + T^-$. Therefore, at large distances, completely different exponents must be used in the wave function to represent electronic configurations corresponding to the above three types of dissociation. The results presented in Table I describe the $He^+ + T$ dissociation which requires opposite signs of β_1 and β_2 in the basis set (33). In Table II we list results obtained for the states that dissociate into $He + T^+$ described by a wave function with the same

signs of β_1 and β_2. The same results are also shown in Fig. 2. The third channel has not been specifically considered by us.

There are no literature data for HeT^+ resonances to compare with. Therefore, we performed a detailed analysis of the small and large R behavior of our results. In those regions it is possible to compare with results of accurate calculations for the atoms obtained in the limit cases. Let us first consider the results presented in Table II and Fig. 2. Because of the exponents used, we should obtain for large R the resonance states of the He atom. Indeed, our lowest eigenvalue is very close to the lowest ^1S resonance state of He whose energy is E = -0.77787 hartree[26]. The two higher eigenvalues approach, respectively, the lowest ^1D and ^1P resonance states of He with energies E = -0.7028 hartree[27] and E = -0.69314 hartree.[26] In Fig. 3 we show the stabilization graph computed at R = 15 bohr with the same type of exponents. The fourth (higher) resonance state corresponds here to the second ^1S resonance state of He (E = -0.62193 hartree).[26] No resonance state, however, is seen in the vicinity of E = -0.59707 hartree,[26] which is the energy of the second ^1P resonance state of helium. Apparently different exponents in the wave function are needed to describe this state.

To further check the large R behavior, we computed with our program the asymptotic values of the energies assuming that the charge Z_1 of the T center is changed from 1 to 0 in the Hamiltonian and using the same expansion of the wave function. Thus, computations for the helium atom have been performed in the elliptic coordinates. These computations have been carried out assuming R = 10.0 and R = 1.0 bohr for the elliptic coordinates. In both cases we obtained results in

full agreement with the above described HeT^+ calculation. The stabilization graph obtained for $Z_1 = 0$ and $R = 1.0$ is shown in Fig. 4. In this case one can also notice the second ^1P state at E = -0.597 hartree, missing in Fig. 3.

As reported earlier[16], similar results had also been obtained for small internuclear distances. With decreasing R the energies of two resonance states of HeT^+ approach the energy of the lowest ^1D and ^1P autoionizing states of Li^+ at E= -1.772 hartree[28] and E = -1.75756 hartree,[26] respectively. As for large R, we performed computations for the united atom system, Li^+, using our trial function in elliptic coordinates, and assuming various distances between centers of coordinates. In all cases consistent results have been obtained. As an example we show in Fig. 5 a stabilization graph obtained for the Li^+ ion assuming R = 1.4 bohr for elliptic coordinates. The energies of the four lowest resonance states are listed in Table III and compared with accurate values.[26,28] It is seen that we reproduced quite accurately the energies of the four lowest resonance states of Li^+.

The above comparison with published results for the atomic cases was made to judge the reliability of our potential energy curves. The very good agreement with the literature data gives us high confidence in our results for the lowest molecular resonances. As a byproduct of our study accurate potential energy curves have been obtained for all the important states of HeT^+ ion. These curves are presented in Fig. 6.

B. PROBABILITIES

The $P_n(q)$ appearing in Eq. (26) has been calculated for each point on the stabilization graph. Within the adiabatic approximation this quantity can be written as[15]

$$P_{nvJ}(q) = (2J + 1)\left[\int_0^\infty S_n^2(R)\, j_J(qR)\, f_{nvJ}^f(R)\, f_0^i(R)\, dR\right]^2 \qquad (34)$$

where n labels now only consecutive electronic states, v and J are the vibrational and rotational quantum numbers, respectively, $j_J(x)$ is the spherical Bessel function, f_{nvJ}^f and f_0^i are the HeT^+ and T_2 radial vibrational wave functions, respectively, and $S_n(R)$ denotes the overlap integral of the electronic wave functions

$$S_n(R) = \int \psi_n^f(\vec{r}_1, \vec{r}_2; R)\, \psi_1^i(\vec{r}_1, \vec{r}_2; R)\, d\vec{r}_1\, d\vec{r}_2 \qquad (35)$$

For the continuous part of the nuclear motion spectrum the expression (34) will not be dependent on v and the vibrational wave function f_{nvJ}^f has to be replaced by a properly normalized continuum wave function $f_{nJ}^f(R|E^f)$. A similar reinterpretation should be made for the continuous part of the electronic spectrum. In our calculations, however, the electronic continuum has been discretized, therefore the formula (35) always holds. In accordance with the common interpretation of the continuum discretization, the probabilities in the continuum represent the total probability connected with a resonance state or with all scattering states within some energy range. They should not be confused with the probability density function, which is not recovered by our method.

In Part II we have presented calculations for all the important discrete electronic states of HeT^+ using the full expression (34). For

the remainder of the spectrum it should be sufficient[15] not to resolve the nuclear motion. Summing/integrating Eq. (34) over v and J, and using a closure relation gives then the following result[29]

$$P_n(q) = \sum_{v,J} P_{nvJ}(q) + \sum_J \int P_{nJ}(q|E)\, dE = \int_0^\infty S_n^2(R)[f_0^i(R)]^2 dR \qquad (36)$$

One may go one step further by assuming that $S_n(R)$ is a slowly varying function of R in the region where $f_0^i(R)$ is nonzero. This gives

$$P_n(q) \approx S_n^2(R_e) \int_0^\infty [f_0^i(R)]^2 dR = S_n^2(R_e) \qquad (37)$$

where R_e is the equilibrium distance in the parent molecule. Eq. (37) means that the overlap integral between the electronic wave functions can serve as a simplest approximation of the probability distribution.

The probability distribution for the lowest discrete electronic states of HeT^+ was given in Part II. For the remaining states we used the expression (36) to obtain the probabilities. This procedure leads to a difficulty in determining the value of ε_n needed in Eq. (31). We adopted for it the difference between the $E_n^f(R)$ energy averaged over R using a formula analogous to Eq. (36) and the $E_1^f(R)$ energy averaged in the same way.

For higher states in the electronic continuum the secular equation root number connected with a given resonance state may vary with R. This was not the case, however, for all the important low lying resonances in the present basis set. Therefore, for all the states considered we identified the electronic level with the root number. This is a justified approximation since, as it will be shown in the next section, high accuracy of this part of the spectrum is not important for determining the neutrino mass.

IV. DEPENDENCE OF THE NEUTRINO MASS ON ACCURACY OF THEORETICAL DATA

Our best probability distribution has been tabulated in Ref. 17. We can estimate the accuracy of the energies and probabilities, and this was done in our previous work.[14-17] However, such estimations do not tell much about the error of a neutrino mass determined using these data. To asses this error we employed the following procedure: (a) Assume that our probability function of Ref. 17 defines a reference system; (b) Construct a β spectrum for a hypothetical neutrino mass (e.g., m_ν = 30 eV); (c) Convolute this spectrum with an experimental resolution function; (d) Generate "experimental" points by the Monte Carlo method with a Gaussian distribution; (e) Fit the obtained spectrum with various model spectra using the least squares method. In this manner we can determine the influence of different approximations, introduced when calculating the model spectra, on the neutrino mass inferred from a β-decay experiment.

A. CONSTRUCTION OF SPECTRA

The calculated $I(E_\beta)$ has to be convoluted with a resolution function according to

$$I_R(E_\beta) = \int I(E') \, R(E', E_\beta) \, dE' \tag{45}$$

Lately the problem of proper determination of the resolution function in a neutrino mass experiment has been the subject of many

discussions.[30-32] It was shown that the use of an inaccurate resolution function to extract the neutrino mass can lead to entirely wrong conclusions. In particular an overestimated width of the resolution function would give too large neutrino mass. The measurement of the resolution function is not easy. In the consecutive IETP group experiments[2,5,6] several aspects of the determination of this function have been modified. For our analysis we have taken their "total" resolution function from Ref. 6. We have fitted this function by the following analytical expression

$$R(E',E_\beta) \equiv R(E' - E_\beta) = \begin{cases} \beta_1 \exp[-\alpha_1 (E' - E_\beta)^2] & \text{for} \quad E' - E_\beta < 0 \\ \beta_2 / [(E' - E_\beta)^2 + \alpha_2^2] & \text{for} \quad 0 < E' - E_\beta \leq 25 \\ \beta_3 / [(E' - E_\beta)^2 + \alpha_3^2] & \text{for} \quad E' - E_\beta \geq 25 \text{ eV} \end{cases} \tag{46}$$

where $\alpha_1 = 0.0051$, $\beta_1 = 0.079$, $\alpha_2 = 24.7$, $\beta_2 = 48.1$, $\alpha_3 = 70.6$, $\beta_3 = 218.8$. Both functions are shown in Fig. 7.

According to Ref. 6, backward scattering causes the resolution function to be constant for $400 < E' - E_\beta < 2500$ eV (see Fig. 1 of Ref. 6). The numerical procedure used by the IETP group to convolute the resolution function truncates, however, this function at some point.[33] Therefore, we decided to truncate the function (46) at some energy as well, and we ignored the above region of constant R. To avoid problems in the fitting process, a Gaussian tail $\exp[-\alpha(E - E_{tr})^2]$ with a small $\alpha = 0.05$ eV^{-2} was added at the truncation point E_{tr}. In addition to the truncated function (46) we have used a resolution function of Fackler et al.[12,34] Preliminary measurements show that the resolution function of their apparatus is Gaussian with

a width of a few electronvolts. We have taken a Gaussian function $(2\pi)^{-1/2}\ \sigma^{-1}\ \exp[-(E'-E_\beta)^2/(2\sigma)^2]$ with σ = 2 eV which corresponds to the width at half height of 4.7 eV.

To obtain the "experimental" data we have to add some statistics to our values. As in Ref. 33, we assumed that for each E_β the statistical error has a Gaussian distribution with standard deviation $\sigma(E_\beta) = \sqrt{I(E_\beta)}$. Since the probability per unit time for a given nucleus to emit a β electron with an energy within, say, a 1 eV bin is very small, this deviation is a good approximation of the actual one. We should note that the error bars shown in Fig. 1 of Ref. 2 and in Fig. 8 of Ref. 33 exhibit a behavior qualitatively different from the one produced by the above formula. Apparently the authors plot something else than they claim in the text.[33] Notice also, that the relative error at each E_β is dependent on the normalization of the spectrum. We have arbitrarily normalized our $I_R(E_\beta)$ to 1000 at 100 eV from the endpoint. The values obtained by fitting the "experimental" spectrum with the model ones, given below, have been obtained, of course, as mean values from several runs with various sequences of random numbers.

The "experimental" spectrum was always generated using our best probability distribution published in Ref. 17. The model spectra were obtained assuming the following decays: bare nuclear, atomic in the two-level model,[7] atomic, and molecular with various levels of accuracy. There are three parameters in each model: m_ν, W_0, and A. In our work we have to choose a value of W_0 for construction of the "experimental" spectrum. The energy W_0 has already been defined as

$$W_0 = M_i c^2 - M_f c^2 - E_R - mc^2 - \Delta E_{11} \qquad (47)$$

In a recent paper Lippmaa et al.[35] measured very accurately the mass difference between the tritium and ^{3}He atoms obtaining $\Delta M = 18599 \pm 2$ eV. Using Eq. (47) this value can be expressed as

$$\Delta M = W_0 + E_R - \Delta E_{11}^{aa} + \Delta E_{11} \qquad (48)$$

ΔE_{11}^{aa} is the difference of the electronic energies of the ^{3}He and T atoms and it is equal to -65.4 eV, for E_R we have taken the standard value of 3 eV, and $\Delta E_{11} = -49.1$ eV. This leads to $W_0 = 18580$ eV. For calculation of the Fermi factor $F(Z, k_e)$ we took $Z = 1$ following Williams and Koonin,[21] i.e. we assumed that the charge of the He nucleus is screened by one electron charge. In the investigated region $F(Z, k_e)$ is almost constant as a function of E, and therefore the choice of Z has practically no influence on our results.

B. RESULTS OF FITS

First we studied the influence of the above mentioned truncation of the resolution function (46) on the determined value of the neutrino mass. We assumed a neutrino mass of 30 eV, integration step of 1 eV and fits were made over a 350 eV range below the endpoint and the nonzero region above it. Various truncations of the function (46) have been used, ranging from 100 eV to the nontruncated function. We have also made calculations taking for construction of the "experimental" spectrum different truncations than for the model one. The fit parameters proved to be very insensitive to the range variations, provided that it was identical for both spectra: changes

in the neutrino mass and W_0 were entirely negligible (~0.01 eV). If, however, the ranges were different, the fit parameters were changing substantially. For example, if the resolution function in the "experimental" spectrum was not truncated whereas it was truncated to 100 eV in the model one, the obtained m_ν and W_0 were 17 and 7 eV too small, respectively. With interchanged ranges, the above values were 17 and 11 eV too large, respectively. As discussed above, the integration in Eq. (45) is truncated during processing of the experimental data.[33] This will lead to a discrepancy between the experimental and model values of the spectra (since the former values naturally contain a contribution from the region neglected in convoluting the latter ones) and in effect to a neutrino mass that is too small.

Our next step was to fit in the various model spectra. The results with the IETP resolution function are presented in Table IV. The shifts from the 30 eV mass for the bare nucleus and the atomic model spectra (23 and 5 eV, respectively) are very similar to those obtained in Ref. 6 when analyzing the valine spectrum with the same models (21 and 4 eV, respectively). The W_0 values also agree well. The atomic two-level model[7] agrees remarkably well with the accurate atomic result. The other results show that with the assumptions employed in Table IV any reasonable molecular tritium spectrum gives a value for the neutrino mass which is very close to 30 eV. The last line in the table represents an attempt to fit our "experimental" spectrum using the identical probability distribution for the model spectrum. The result is not exactly equal to 30 eV because of random deviations in the sample. All the data in Table IV were obtained on

the same series of sets of random numbers. The differences between various models are well preserved even in a single Monte Carlo run. The neutrino mass is the parameter most sensitive to the Monte Carlo sampling. In Table IV we give also the results of runs without statistical deviations added in the "experimental" spectrum (but with the same weights as above). The values agree within the error bounds with the Monte Carlo results, with a shift of ~0.1 eV towards larger neutrino mass.

In Table V we present analogous results with a Gaussian resolution function of a 4.7 eV width. Conclusions similar to those drawn from Table IV apply to these results. The only notable difference is that the fitted $m_{\bar{\nu}}$ for the bare nucleus model spectrum is now about 6 eV larger. With this resolution function the neutrino mass from a run without the statistical deviation is 0.1 - 0.3 eV smaller than the Monte Carlo value.

We tested the importance of the approximation introduced by Eq. (17). To this end we took probabilities obtained from a 200-term wave function used for the stabilization method calculation for a fixed R = 1.4 bohr, decreased the probability for the ground state by 0.2%, and increased the probability for the first excited state by the same amount (c.f. Ref. 21). As shown in Tables IV and V, this procedure led to the same value of the extracted neutrino mass (within 0.1 eV) indicating sufficiently high accuracy of the present theoretical formula.

To show the accuracy of our basis sets we used for construction of the model spectrum the probability distribution[36] obtained with relatively poor configuration interaction (CI) expansion in s and p

Gaussian type orbital (GTO) basis set. This represents a standard quantum chemical calculation and it is similar to the latest work by Kaplan et al.[9] The obtained results should be compared with our R = 1.4 bohr results. Tables IV and V show that the agreement is quite good. Therefore such calculations are entirely adequate if the neutrino mass is to be determined with a few eV accuracy.

Let us now discuss the effect of nuclear motion. From Tables IV and V we see that all our molecular spectra lead to almost identical neutrino masses. The nuclear motion effects produce ~1.5 - 1.8 eV shift of the endpoint energy. This could be predicted because of the characteristic change of the shape of Kurie plots at the endpoint discussed by us in Ref. 17. The above shift is related to the ~1 eV spacing between the final plot and the plots representing calculations without including the nuclear motion.

The resolution function (46) has about 36 eV width at half height. To check how an under/overestimation of the width can influence the results we constructed two functions similar to the function (46) but of 45 and 25 eV width. All the parts of the function (46) have been proportionally contracted or expanded. The results shown in Table VI indicate that this effect may be smaller than expected.[30-32] The changes in both the neutrino mass and the endpoint energy are not larger than 5 eV even in the most drastic case when the widths for the "experimental" and model spectra differ by 20 eV.

The almost identical values of the neutrino mass obtained with very different molecular model spectra clearly point out that the probability distribution in the shake-off region cannot have any significant influence on the results. To make it even more certain we

performed calculations with a probability distribution obtained from our final probability distribution[17] by binning the values lying above the ionization limit. Bins of 1 and 10 eV width have been used. The two obtained model spectra led to deviations of about 0.01 and 0.1 eV, respectively, in both the neutrino mass and the endpoint energy.

All the above calculations have been performed with the neutrino mass equal to 30 eV in the "experimental" spectrum. Table VII shows results of the same type calculations for a 1 eV mass. Since the two resolution functions produced almost identical conclusions above, we restricted the calculations to the Gaussian resolution function of 4.7 eV width. We observe that accuracy of the theoretical model is now much more important. The less accurate models, including the GTO CI molecular calculation, predict zero mass. If the nuclear motion effects are not included, the mass is 0.6 eV too small. Inclusion of the nuclear motion in an average way leads to almost twice too large neutrino mass. This shows that the effects of the nuclear motion are crucial for determining the neutrino mass if it is of the order of 1 eV.

Let us point out that it is very important that the resolution function is rapidly falling off for small E_β. Let us consider the expression (45) for $E_\beta = W_0$ and a Lorenzian resolution function. This function behaves as $(E' - W_0)^{-2}$ in the tail while $I(E') \sim (E' - W_0)^2$ in a large region below the endpoint. Therefore, the integrand in Eq. (45) is constant in this region, which causes the integral to be quasidivergent. It is not really divergent due to the standard shape of the β spectrum. To compute this integral we had to now integrate up to $E' = 0$. From the practical point of view this means that, due to

the resolution, the number of events at $E_\beta = W_0$ is mainly defined by the value of I for E′ hundreds of electronvolts from the endpoint. Clearly, it would be hard to believe that any experiment can be sensitive to a small effect near the endpoint if the resolution changes the actual spectrum so drastically. We made some runs with a long-tail resolution function finding that the results are extremely sensitive to truncations of this tail. An approach similar to ours was taken by Law.[37] He used, however, a resolution function Lorenzian in p. With this choice, all the problem discussed above becomes even more severe.

V. SOLID STATE EFFECTS

The results presented above refer to gaseous T_2. One can show,[38] however, that in the case of frozen T_2, as used in the experiment of Ref. 12, the fractional change of the T_2 wave function, $\Delta\psi/\psi$, caused by the binding in the crystal lattice, amounts to less than 0.1%. On the other hand, the final states of the system may be more effected by the solid state surrounding than the initial state. Wagner and Taylor[39] performed a CS_2 experiment which found an energy shift of 2 eV due to the charge - induced dipole interactions in the solid. Let us assume for a moment that the effect is of the same order for the beta decay in solid T_2. The above interaction leads to a shift of comparable size for all the low lying states of HeT^+. The final effect on the neutrino mass will be much smaller than 2 eV since had the shifts been identical for all the levels, it would have had no effect on the neutrino mass.

We can easily estimate the actual value of the above discussed shift for HeT^+ and for CS_2. The effect depends on the distances between molecules in a solid, which are about 1.5 times larger for CS_2 than for T_2, and on the polarizability of a molecule, which is 10 times larger for CS_2 than for T_2. A simple calculation based on the multipole expansion shifts the energy by about 0.8 eV and 3.6 eV for HeT^+ and CS_2, respectively. The latter value is in a good agreement with the one obtained in the Wagner and Taylor[39] experiment. A more elaborate calculation could lead to a somewhat different value, particularly for CS_2. This is because in the x-ray photoemission the system changes from a closed-shell to an open-shell one while in the

case of β decay the shell structure does not change. It is well known that the interaction of closed-shell systems is much weaker than that involving open shells. Also the overlap between molecules is much larger for CS_2. It seems that any possible estimation of the effect of the solid state surrounding is much smaller than 1 eV and therefore our results can be applied for the solid T_2 experiment of 1 eV accuracy.

To support the above conclusions we give here a more detailed description of the estimation of the solid state energy shifts. The crystal structure of CS_2 has been recently reinvestigated by Powell et al.[40] They found that the crystal is orthorhombic Cmca (D18/2h) with four molecules in a cell. The molecules are in layers parallel to the bc plane and are tilted by an angle ϕ = 48 degree with respect to the b axis. The lattice parameters are a = 6.1, b = 5.3 and c = 9.4 Å. Williams and Amos[41] calculated various properties of CS_2 using SCF and MCSCF methods. The polarizability α was obtained only by finite field SCF but its value 54.0 a.u. [1 a.u. of polarizability = $e^2a_0^2E_h^{-1}$ = 1.6488 (-41) F m^2] agrees well with the value 55.2 a.u. which Williams and Amos extracted from an experiment by Bogaard.[42] The interaction of the charge on CS_2^+ or HeT^+ with the induced dipoles can be easily estimated from the multipole expansion as $-\alpha R_1^{-4}/2$, where R_1 is the distance between molecules. For the crystal this value has to be multiplied by a lattice factor. This factor for the fcc structure of T_2 is 25.[43] The value of the factor for the CS_2 crystal structure is unknown and therefore in all the calculations the same value of 25 was used. For H_2 at R = 1.4 bohr the parallel and perpendicular components of α are 6.380 and 4.578 a.u., respectively.[44] Taking the isotropic α

= 5.17 a.u. and R_1 = 6.79 bohr (R_1 is the distance between centers of molecules in the solid D_2; we could not find this value for T_2 but it will be slightly smaller) leads to an energy shift of 0.83 eV. If we take for CS_2 the R_1 value as an average of the three distances given above R_1 = [(a+b/2+c/2)/3] = 8.5 a.u., we get 3.6 eV for the shift.

Another possible effect peculiar to crystals could be the recoilless β decay of a T_2 molecule. If this happens, a corresponding shift of E_β occurs to higher values by the amount of the recoil energy E_R. Such events, if occurring significantly, could seriously change the β spectrum. However, we will show that these events can be safely ignored.

The phenomenon considered is reminiscent of the Mössbauer effect[45] involving the recoilless γ emission of heavy nuclei that are embedded in crystals. The theory of this effect is reviewed in a classic article by Boyle and Hall.[46] Qualitatively a recoilless emission can only take place if the decaying system is quite rigidly bound to the bulk crystal. This is clearly possible in Mössbauer spectroscopy but seems impossible for T_2 crystal since the molecular crystal binding energy of about $3 \cdot 10^{-3}$ eV is only a tiny fraction of the recoil energy E_R = 3 eV.

To arrive at a more quantitative measure we start from the Heisenberg uncertainty principle. Quantum mechanically a single T_2 molecule is a subsystem of the entire crystal and therefore, strictly speaking, it will not be in a definitive eigenstate. Yet we can associate a localization width of the molecule which will be of the order of the lattice spacing

$$\Delta x \sim R_1 \approx 6.5 \text{ bohr} \tag{49}$$

The corresponding spread in the T_2 CM momentum is therefore

$$\Delta p \sim \hbar/\Delta x \approx 0.15 \text{ a.u.} \tag{50}$$

However, the recoil momentum associated with a β decay is $p_\beta = (2E_\beta)^{1/2} \approx 37$ a.u., which is well beyond the spread of Eq. (50). According to the theory,[46] the probability of the recoilless emission is given by the Debye-Waller factor. Assuming an essentially Gaussian localization of the T_2 molecule, this factor is found to have the form[46]

$$f = \exp(-p_\beta^2 \langle x^2 \rangle) \tag{51}$$

where $\langle x^2 \rangle$ is the mean square of the deviation of T_2 from the equilibrium position

$$\langle x^2 \rangle \sim (\Delta x/2)^2 \approx 10 \text{ bohr}^2 \tag{52}$$

Therefore $f \sim 10^{-5945}$, a very small number indeed, which indicates that the recoilless β decay can be ignored.

Once the emitted β electron has left the vicinity of the daughter molecule, multiple scattering off other T_2 molecules in the solid source can occur. Inelastic collisions can absorb a significant amount of kinetic energy of the β electron, which could cause a discernible smearing of the β spectrum. One way to eliminate this effect experimentally is by the use of various thicknesses of the (layered) source - up to several hundred layers will be considered. Since a thin film sample will contain relatively few layers and the e-T_2 inelastic scattering cross-section is quite small, we expect the multiple scattering to cause only very small energy losses in this case. However, the quantitative details are lacking and we are investigating them following methods developed earlier.[47]

VI. DISCUSSION AND CONCLUSIONS

The various approximations made in the derivation of the T_2 β-decay spectrum of Eq. (32) have been pointed out in Sec. II. Our treatment has been basically nonrelativistic but we used a correct relativistic relations to describe the kinematics of the β electron and the antineutrino, which should at present be entirely sufficient for the process considered. The relativistic effects are expected to be negligible.[4] The problem may, however, require investigation if the neutrino mass happens to be very small.

Due to the weakness of the weak interaction the restriction to first order in the interaction in Eq. (2) should not lead to any observable error. The same is true for the assumption of the independence of the internal nuclear and molecular motions and of the localization of the internal nuclear wave function. The first nonnegligible approximation is introduced by Eq. (17). On the basis of Williams and Koonin's[21] results for the atomic tritium we may expect this effect to be about 0.2% in the transition probabilities to the lowest electronic states. As shown in Sec. IV, such error can lead to an overestimation of the neutrino mass by less than 0.1 eV for the true neutrino mass equal to 30 eV. Williams and Koonin have also found that the correction due to the exchange of the β electron with the molecular ones should be smaller by a factor η^2 ($\approx 0.027^2$) than the above correction and therefore negligible.

Another approximation was the use of the adiabatic form for the molecular wave functions of T_2 and HeT^+. For these systems this approximation is known[48] to lead to results which differ negligibly

from those obtained in the complete nonadiabatic treatment. The possible errors will be definitely smaller than those introduced by the inaccuracies of the present basis set expansions of the wave functions (see below).

We also assumed that in the probability $P_n(q)$ the value of q, which is proportional to the length of the vector representing the sum of the β electron and antineutrino momenta, is independent of the latter momentum. Furthermore, in our calculations of P_n we took for q a constant value such that $2q^2 = 18.6$ keV. This should be a good approximation in the region close to the endpoint, as investigated. We have found that the value of $P_n(q)$ was quite insensitive to the changes in q^2 of the order of 100 eV.

The probabilities P_n and the energies E_n have been calculated with some numerical errors. We were able to reduce most of these errors to an insignificant level. High accuracy of the electronic bound states has been demonstrated in Part I: the error of S_n^2 was determined to be of the order of 0.0001 and the error of E_n of the order of 0.0001 eV. The equations for the nuclear motion have been solved accurately enough to introduce no additional error, which was checked by employing various sum rules.[15] Therefore we believe that the error of our value of the probability P_{nvJ} is determined by the error of $S_n^2(R)$, at least for $n = 1$. For the excited electronic states of HeT^+ the relative error might be somewhat larger since the adiabatic correction for the nuclear motion has not been included in our calculations. The total probability connected with these states is, however, smaller than the probability of transitions to the ground electronic state, so that the absolute error should not be larger than

the one estimated above. Since the electronic states 1-4 and 6, for which the nuclear motion in $^3HeT^+$ has been considered, give 84.2% of the probability, and affect the most important part of the β spectrum, it is entirely sufficient for the remaining states to account for the nuclear motion in the averaged manner according to Eq. (36).

The accuracy of the electronic resonance states is lower, and there is a small arbitrariness in the positions of the states. Since most of the transition probability in the spectrum above the ionization threshold is connected with the resonances, this could in principle lead to some inaccuracies. We have found, however, (see Sec. IV) that even drastic changes of both the energies and transition probabilities caused by binning the values in the shake-off region have practically no effect on our final result.

Recently Martin and Cohen[49] calculated the Kurie plots for the β decay of T_2 using the so called Stieltjes imaging technique[50] for the continuum states. This technique provides continuous probability distribution from a computation that produces a discrete spectrum. Although Martin and Cohen's approach to the continuum is formally more advanced than the one used in the present work, their results in the shake-off region do not need to be more accurate than ours. There are two reasons for this. First, these authors performed calculations only for R = 1.4 bohr, which cannot be adequate for the states which are of a strongly repulsive character in the region of interest. Second, they base their analysis on the discrete spectrum resulting from diagonalization of a Hamiltonian matrix which is of much poorer quality than ours. The Stieltjes treatment leads to a continuous probability density function which is shifted to lower energies

compared to our results. One can also infer from their Fig. 1b that most of the probability in this region comes from a ~10 eV wide resonance in the region of 60 - 70 eV. Our results described in Sec. III show that this probability is connected with two resonances separated by about 7 eV. We have performed calculations[51] of these resonances widths by analytical continuation of stabilization graphs. These calculations showed[51] that both resonances are narrow, having the widths of about 0.1 eV. Although the probability distribution in the shake-off region is of importance for physical chemistry, we have shown in Sec. IV that its precise knowledge is fortunately not important for the neutrino mass determination.

If the neutrino mass is 30 eV, even relatively poor molecular calculations for a single internuclear distance are good enough for determination of this mass. Therefore, the Kaplan et al.[9] calculations for valine should be appropriate for analyzing the IETP experiment.[6] The situation is quite different for a 1 eV neutrino mass. The less accurate calculations would lead to zero neutrino mass in this case. There are, of course, two kinds of molecular effects that influence the neutrino mass determination: the effects of molecular binding and the effects of the nuclear motion within molecules. Even very accurate calculations which include only the former effects, i.e. calculations for a fixed internuclear distance, would not be adequate for a 1 eV mass. We showed in Ref. 17 that in the vicinity of the endpoint (last ~3 eV) the latter effects, which had not been considered before, introduce a qualitative change of the shape of the β spectrum. Due to the spread of the final rovibrational levels in the ground electronic state, the final theoretical Kurie plot close to the endpoint is

practically tangent to the energy axis. This is to be compared with the pure nuclear or atomic decay where the plot is essentially perpendicular to the energy axis. This phenomenon does not appear in a molecular calculation which neglects the nuclear motion in the daughter molecular ion. If the neutrino mass is of the order of 1 eV or smaller accounting for this effect is crucial.

Solid state effects other than possible β electron energy losses due to e-T_2 inelastic scattering have been found negligible. A quantitative study of these losses will be a subject of a forthcoming study.

The analysis of Section IV sheds also some light on the question of the resolution function as used in the IETP experiments.[2,5,6,33] Our results show that the effect of overestimation of the width of resolution function may be somewhat smaller than suggested before.[30-32] On the other hand, we show that truncation of the resolution function, as employed in processing of the experimental data,[33] may introduce some additional inaccuracies.

ACKNOWLEDGMENTS

This work was performed by Lawrence Livermore National Laboratory under the auspices of the U.S. Department of Energy under grants No. W-7405-ENG-48 and DE-FG05-85ER13447. It was also supported in part by grants from National Science Foundation No. CHE-8207220, University of Florida DSR, and Polish Academy of Sciences No. MR.I.9. We thank the Particle Physics Group at Rockefeller University and Dr. E. Clementi's group at IBM in Kingston for providing access

to their computational facilities. We are also indebted to Drs. K.E. Bergkvist, J. Law, J.J. Simpson, and L.Z. Stolarczyk for valuable discussions.

CAPTIONS TO FIGURES

Fig. 1. HeT^+ energies at R = 1.4 bohr as functions of the scaling parameter.

Fig. 2. Energies of some HeT^+ resonance states as functions of R calculated with exponents corresponding to the dissociation into He + T^+. The He atom resonance states energies shown on the right axis are from Refs. 26 and 27.

Fig. 3. HeT^+ energies at R = 15 bohr as functions of the scaling parameter calculated with exponents corresponding to the dissociation into He + T^+. The He atom resonance states energies shown on the right axis are from Refs. 26 and 27.

Fig. 4. He energies obtained from calculations in the basis set (33) with Z_1 = 0 and R = 1.0 bohr as functions of the scaling parameter. The He atom resonance states energies shown on the right axis are from Refs. 26 and 27.

Fig. 5. Li^+ energies obtained from calculations in the basis set (33) with Z_1 = 0, Z_2 = 3, and R = 1.4 bohr. The He atom resonance states energies shown on the right axis are from Refs. 26 and 28.

Fig. 6. Energy curves for HeT^+.

Fig. 7. The resolution function from Ref. 6 (broken line) and the fit of Eq. (46) (solid line).

Fig. 8. The β spectrum of the tritium molecule and the same spectrum convoluted with a Lorenzian resolution function of 20 eV width.

REFERENCES

1. F. Reines, H.W. Sabel, and E. Pasierb, Phys. Rev. Lett. 45, 1307 (1980).
2. V. A. Lubimov, E. G. Novikov, V. E. Nozik, E. F. Tretyakov, and V. S. Kosik, Phys. Lett. B 94, 266 (1980).
3. F. Boehm and P. Vogel, Ann. Rev. Nucl. Sci. 34, 125 (1984).
4. Ching Cheng-riu and Ho Tso-hsiu, Phys. Rep. 112, 1 (1984); Ching Cheng-riu, Ho Tso-hsiu, and Chao Hsiao-lin, Commun. Theor. Phys. 1, 267 (1982).
5. S. Boris, A. Golutvin, L. Laptin, V. Lubimov, V. Nagovizin, E. Novikov, V. Nozik, V. Soloshenko, I. Tichomirov, E. Tretiakov, manuscript, Moscow 1983; see also S. Boris et al. in Proceeding of the International Europhysics Conference on High Energy Physics, Brighton, 1983, ed. by J. Guy and C. Costain (Rutherford Appelton Laboratory, Chilton, Didcot, UK, 1984), p. 386.
6. S. Boris, A. Golutvin, L. Laptin, V. Lubimov, V. Nagovizin, E. Novikov, V. Nozik, V. Soloshenko, I. Tihomirov, and E. Tretjakov, Phys. Lett. B 159, 217 (1985).
7. K. E. Bergkvist, Phys. Scr. 4, 23 (1971); Nucl. Phys. B 29, 317, 371 (1972).
8. I. G. Kaplan, V. N. Smutny, and G. V. Smelov, Phys. Lett. B 112, 314 (1982); Sov. Phys. JETP 57, 483 (1983),[Zh. Eksp. Teor. Fiz. 84, 833 (1983)].
9. I.G. Kaplan, G.V. Smelov, and V.N. Smutny, Dokl. Akad. Nauk USSR 279, 1110 (1984).

10. J.J. Simpson, Phys. Rev. D 23, 649 (1981).

11. Massive Neutrinos in Astrophysics and in Particle Physics, Proceedings of the Fourth Moriond Workshop, La Plagne-Savoie, France 1984, ed. by J. Tran Thanh Van (Edition Frontiers, Paris).

12. O. Fackler, M. Mugge, H. Sticker and R. Woerner, in Ref. 11, p. 281.

13. R. G. H. Robertson, T. J. Bowles, J. C. Browne, T. H. Burritt, J. A. Hollfrich, D. A. Knapp, M. P. Maley, M. L. Stelts, and J. F. Wilkerson, in Ref. 11, p. 253.

14. W. Kołos, B. Jeziorski, K. Szalewicz, and H. J. Monkhorst, Phys. Rev. A 31, 551 (1985).

15. B. Jeziorski, W. Kołos, K. Szalewicz, O. Fackler, and H. J. Monkhorst, Phys. Rev. A 32, 2573 (1985).

16. W. Kołos, B. Jeziorski, H. J. Monkhorst, and K. Szalewicz, Intern. J. Quantum Chem. S 19, 000 (1985).

17. O. Fackler, B. Jeziorski, W. Kołos, H.J. Monkhorst, and K. Szalewicz, Phys. Rev. Lett. 55, 1388 (1985)

18. C.S. Wu and S.A. Moszkowski "Beta Decay", Wiley, New York, 1966, ch. 2.; E.J. Konopinski, "The Theory of Beta Radioactivity", Claredon Press, Oxford, 1966.

19. E.G. Harris "A Pedestrian Approach to Quantum Field Theory", Wiley, New York, 1972, p.78.

20. A. Messiah, "Quantum Mechanics", North-Holland, Amsterdam, 1961, vol. I, p. 484.

21. R. D. Williams and S. E. Koonin, Phys. Rev. C 27, 1815 (1983).

22. H.M. Schwartz, J. Chem. Phys. 23, 400 (1955)

23. M. Cantwell, Phys. Rev. 101, 1747 (1956).

24. F. N. D. Kurie, J. R. Richardson, and H. C. Paxton, Phys.

Rev. 49, 368 (1936).

25. E. Holoien, Proc. Phys. Soc. A 71, 357 (1958); H. S. Taylor, G. V. Nazaroff, and A. Golębiewski, J. Chem. Phys. 45, 2872 (1966); H. S. Taylor, Adv. Chem. Phys. 18, 91 (1970).
26. Y.K. Ho, Phys. Rep. 99, 1 (1983); Phys. Rev. A 23, 2137 (1981).
27. A.K. Bathia and A. Temkin, Phys. Rev. A 11, 2108 (1975).
28. A.K. Bathia, Phys. Rev. A 15, 1315 (1977).
29. L. Wolniewicz, J. Chem. Phys. 43, 1087 (1965).
30. J.J. Simpson, Phys. Rev. D 30, 1110 (1984).
31. K.E. Bergkvist, Phys. Lett. B 154, 224 (1985).
32. K.E. Bergkvist, Phys. Lett. B 159, 408 (1985).
33. V.A. Lubimov, E.G. Novikov, V.Z. Nozik, E.F. Tretiakov, V.S. Kozik, and N.F. Myasoedov, Sov. Phys. JETP 54, 616 (1981), [Zh. Eksp. Teor. Fiz. 81, 1158 (1981)].
34. O. Fackler, M. Mugge, H. Sticker, and R. Woerner, to be published.
35. E. Lippmaa, R. Pikver, E. Suurmaa, J. Past, J. Puskar, I. Koppel, and A. Tammik, Phys. Rev. Lett. 54, 285 (1985).
36. O. Fackler and N. Winter, unpublished, and O. Fackler, M. Mugge, H. Sticker, N. Winter, and R. Woerner, in Ref. 9, p. 373.
37. J. Law, Phys. Lett. B 102, 371 (1981).
38. L.Z. Stolarczyk and H. J. Monkhorst, unpublished.
39. C.D. Wagner and J.A. Taylor, J. Electron Spectr. 28, 211 (1982).
40. B.M. Powell, G. Dolling, and B.H. Torrie, Acta Cryst. B 38, 28 (1982).
41. J.H. Williams and R.D. Amos, Chem. Phys. Lett. 66, 370 (1979).
42. M.P. Bogaard, A.D. Buckinghan, R.K. Pierens, and A.H. White Trans.

Faraday Soc. I 74, 3008 (1978).

43. "Rare gas solids", ed. by M.L. Klein and J.A. Venables, Academic, London 1976, vol. 1, p. 154.

44. W. Kołos and L. Wolniewicz, J. Chem. Phys. 46, 142 (1967).

45. R.L. Mössbauer, Z. Phys. 151, 124 (1958); Naturwissenschaften 45, 538 (1958); Z. Naturforsch. 14a, 211 (1959); Ann. Rev. Nucl. Sci. 12, 123 (1962).

46. A.J.F. Boyle and H.E. Hall, Rept. Progr. Phys. 25, 1 (1962).

47. W. Kołos, H.J. Monkhorst and K. Szalewicz, J. Chem. Phys. 77, 1323, 1335 (1982); At. Nucl. Data Tables 28, 239 (1983); K. Szalewicz, W. Kołos, H.J. Monkhorst and C. Jackson, J. Chem. Phys. 80, 1435 (1984).

48. D. M. Bishop and L. M. Cheung, Adv. Quantum Chem. 12, 1 (1980).

49. R. L. Martin and J. S. Cohen, Phys. Lett. A 110, 95 (1985).

50. P.W. Langhoff, C.T. Corcoran, J.S. Sims, F. Weinhold, and K.M. Glover, Phys. Rev. A 14, 1042 (1976).

51. B. Jeziorski, P. Froelich, W. Kołos, H.J. Monkhorst, and K. Szalewicz, presented at 19th Quantum Chemistry Symposium at Marineland, Florida, March 1985, and to be published.

Table I. Energies of a few lowest resonance states of HeT^+ (hartree). For large R the exponents in the wave function correspond to the dissociation into $He^+ + T$

R	Energy						
	1	2	3	4	5	6	7
0.4	3.164	3.223	3.258	3.415	3.59		
0.5	2.145	2.228	2.271	2.435	2.585		
0.6	1.445	1.553	1.622	1.792	1.89	1.90	
0.8	0.53	0.685	0.842	0.99	1.01	1.02	1.04
0.9	0.21	0.39	0.59	0.68	0.72	0.74	0.77
1.0	-0.05	0.15	0.390	0.410	0.440	0.450	0.563
1.2	-0.43	-0.205	0.063	0.095	0.116	0.123	0.278
1.4	-0.69	-0.455	-0.208	-0.183	-0.177	-0.097	0.081
2.0	-1.055	-0.825	-0.591	-0.571	-0.562		
3.0	-1.1405	-0.9973	-0.7659	-0.7361	-0.7258		
4.0	-1.0949	-1.0140	-0.8105	-0.7476	-0.7418	-0.685	
5.0	-1.0452	-1.0089	-0.8225	-0.746	-0.736	-0.733	
6.0	-1.0161	-1.0045	-0.8188	-0.777	-0.737	-0.729	
7.0	-1.0048	-1.0022	-0.8036	-0.785	-0.737	-0.725	
8.0	-1.0014	-1.0012	-0.7836	-0.7235	-0.7219	-0.6622	
10.0	-1.0004	-1.0002	-0.7474	-0.7226	-0.7219	-0.6802	

Table II. Energies of some resonance states of HeT^+ (hartree). The exponents in the wave function correspond to the dissociation into $He + T^+$.

R	Energy		
7.0	-0.782	-0.745	-0.678
8.0	-0.780	-0.735	-0.682
9.0	-0.780	-0.730	-0.685
10.0	-0.782	-0.725	-0.688
12.0	-0.780	-0.713	-0.690
15.0	-0.780	-0.709	-0.692

Table III. Energies of the Li^+ ion (hartree) computed using a 200-term expansion in elliptic coordinates (R = 1.4 bohr).

State	Energy	
	present	Refs. (26, 28)
$^1S(1)$	-1.905	-1.90585
$^1D(1)$	-1.766	-1.772
$^1P(1)$	-1.756	-1.75756
$^1S(2)$	-1.629	-1.63044

Table IV. Effect of various model spectra on the neutrino mass. The molecular R = 1.4 and R-averaged spectra were constructed from 200-term wave functions using 100 lowest eigenstates. The resolution function of Eq. (46) has been used. The assumed neutrino mass in the "experimental" spectrum was 30 eV. Fits were made over a 400 eV range with 50 eV above the endpoint. The integration step was 1 eV. The numbers in parenthesis denote the RMS of the mean from a series of Monte Carlo runs. The lower numbers are from a non Monte Carlo calculation. All values are in eV.

model spectrum	m_ν	W_0
bare nucleus	6.4 (0.3)	18561.8 (0.05)
	6.7	18561.8
two-level atomic	25.5 (0.2)	18573.9 (0.07)
	25.6	18573.9
atomic	25.2 (0.2)	18573.7 (0.07)
	25.3	18573.7
GTO CI, Ref. 36	29.2 (0.2)	18577.6 (0.08)
	29.3	18577.7
molecular R=1.4 bohr, 200-term	30.0 (0.2)	18578.2 (0.08)
	30.1	18578.3
same as above but with 0.2% change of two lowest probabilities	30.0 (0.2)	18578.3 (0.08)
	30.1	18578.3
molecular R-averaged	30.2 (0.2)	18578.5 (0.08)
	30.3	18578.5
final	29.9 (0.2)	18580.0 (0.08)
	30.0	18580.0

Table V. Effect of various model spectra on the neutrino mass with a Gaussian resolution function of 4.7 eV width. The remaining assumptions were the same as in Table IV.

model spectrum	m_ν	W_0
bare nucleus	12.3 (0.1) 12.2	18562.5 (0.05) 18562.5
two-level atomic	25.4 (0.1) 25.2	18573.9 (0.07) 18573.8
atomic	25.3 (0.1) 25.0	18573.8 (0.06) 18573.6
GTO CI, Ref. 36	29.3 (0.1) 29.1	18577.7 (0.07) 18577.6
molecular R=1.4 bohr, 200-term	30.0 (0.1) 29.7	18578.3 (0.07) 18578.2
same as above but with 0.2% change of two lowest probabilities	30.0 (0.1) 29.8	18578.4 (0.07) 18578.2
molecular R-averaged	30.3 (0.1) 30.0	18578.6 (0.07) 18578.5
final	30.2 (0.1) 30.0	18580.1 (0.06) 18580.0

Table VI. Effect of using resolution functions of different widths. The results presented are from a non Monte Carlo calculations. The remaining assumptions were the same as in Table IV.

Width ("experimental"/model)	$m_{\tilde{\nu}}$	W_0
36/36	30.0	18580.0
45/36	29.5	18582.5
36/25	28.4	18582.4
45/25	27.8	18584.8
36/45	31.8	18577.8
25/36	33.0	18578.0
25/45	33.2	18575.2

Table VII. Effect of various model spectra on the neutrino mass with a Gaussian resolution function of 4.7 eV width. The neutrino mass used in the "experimental" spectrum was 1 eV. The integration step was 0.1 eV. The remaining assumptions were the same as in Table IV.

model spectrum	$m_{\bar{\nu}}$	W_0
bare nucleus	0.00	18567.19
atomic	0.00	18575.38
GTO CI, Ref. 36	0.00	18577.91
molecular R=1.4 bohr, 200-term	0.40	18578.22
molecular R-averaged	1.92	18578.45
final	1.00	18580.00

FIGURE 1

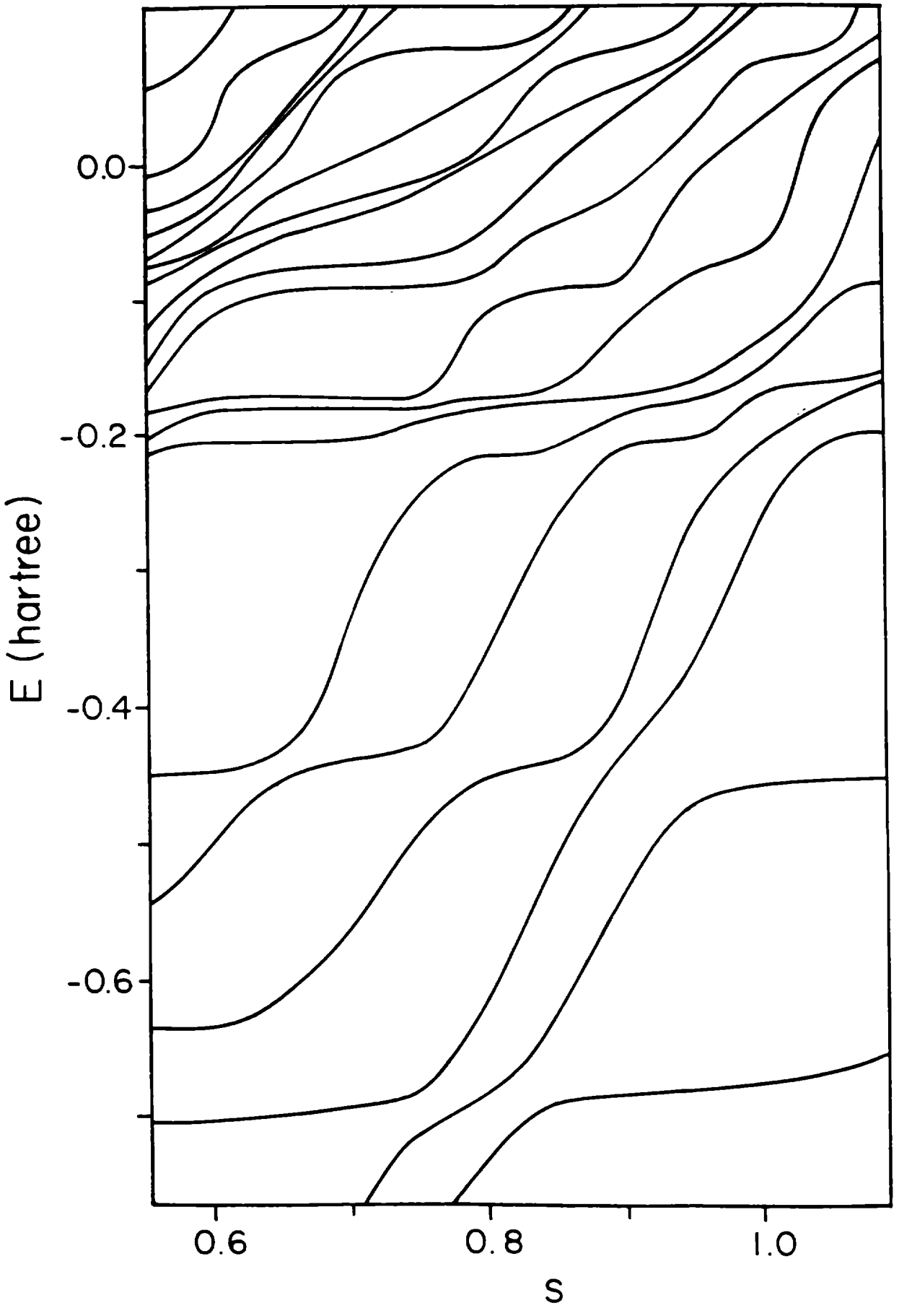

FIGURE 2

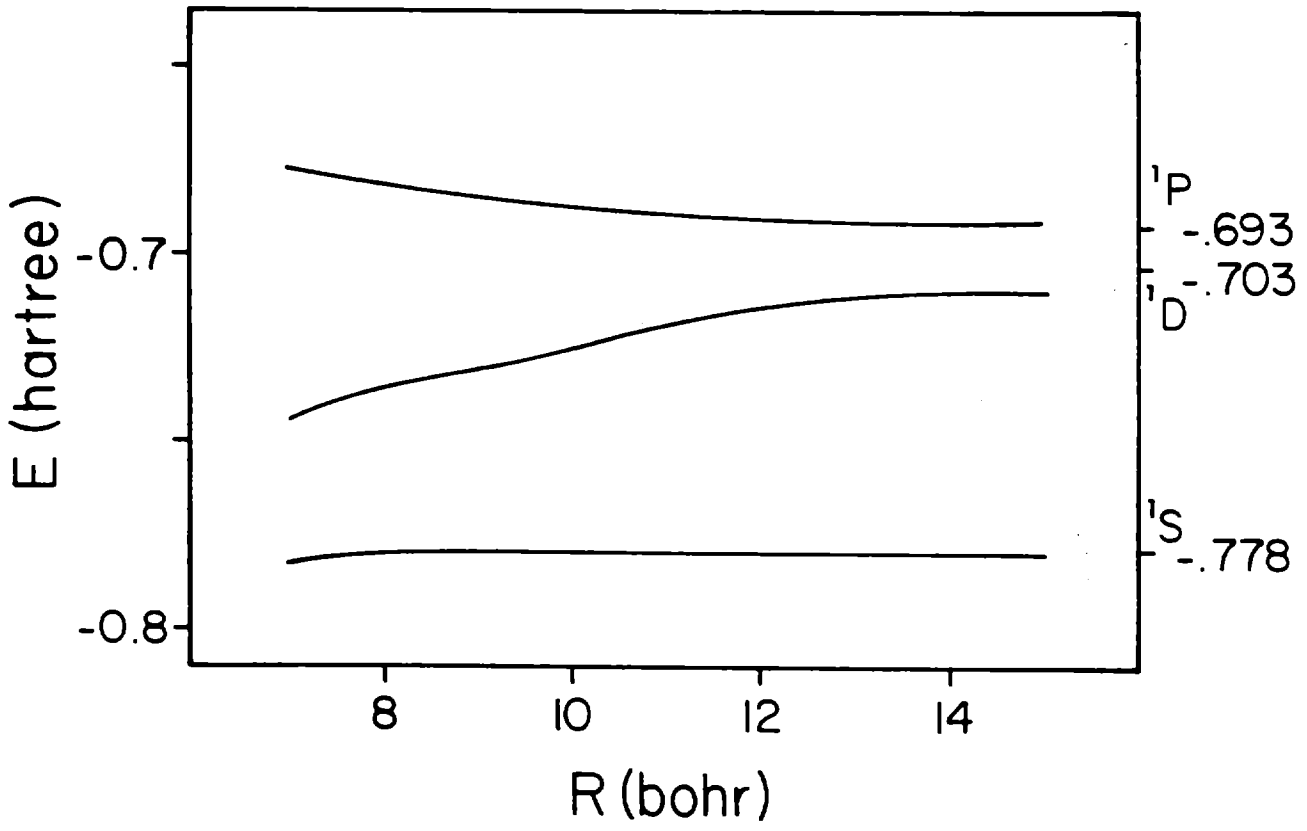

FIGURE 3

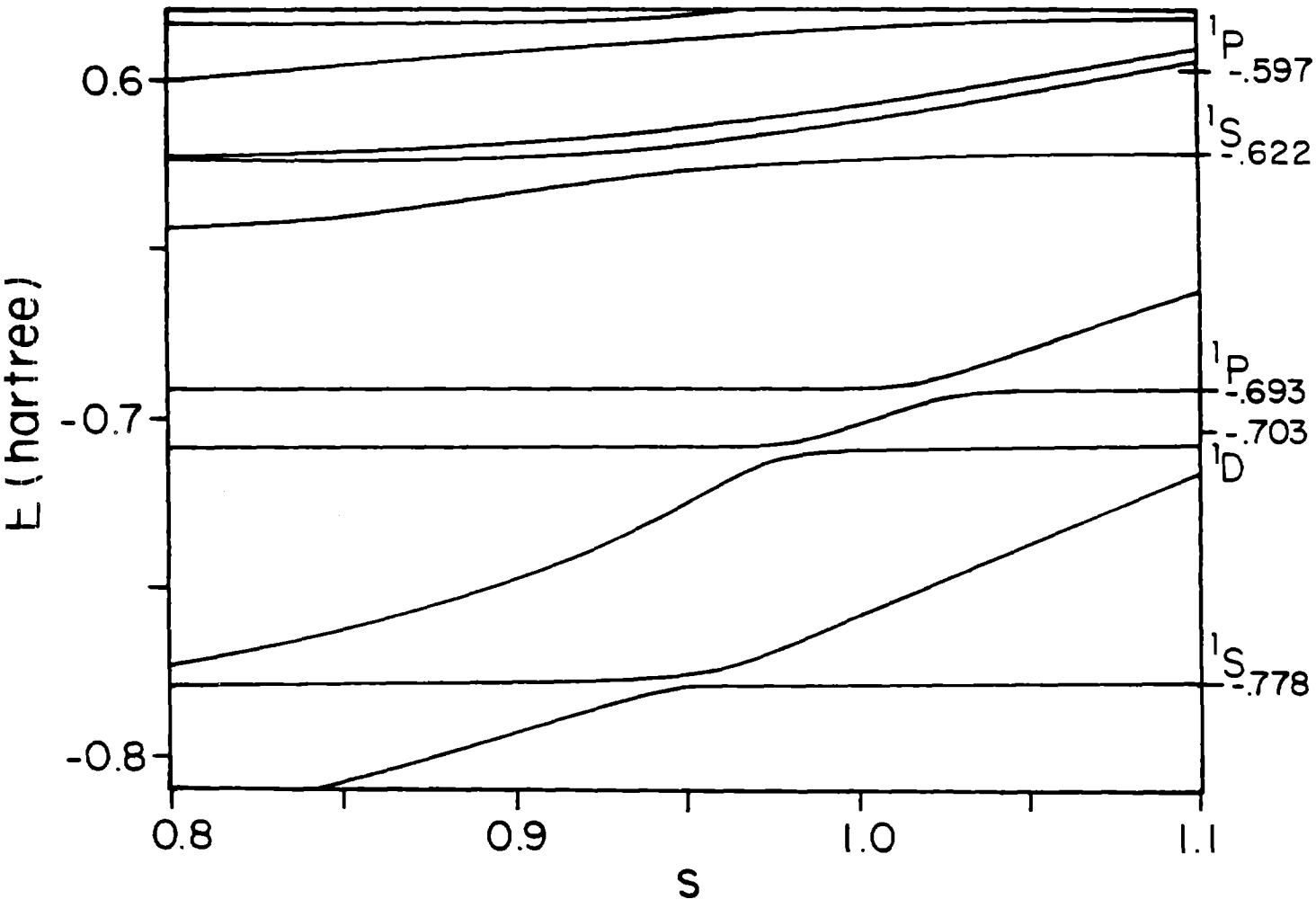

FIGURE 4

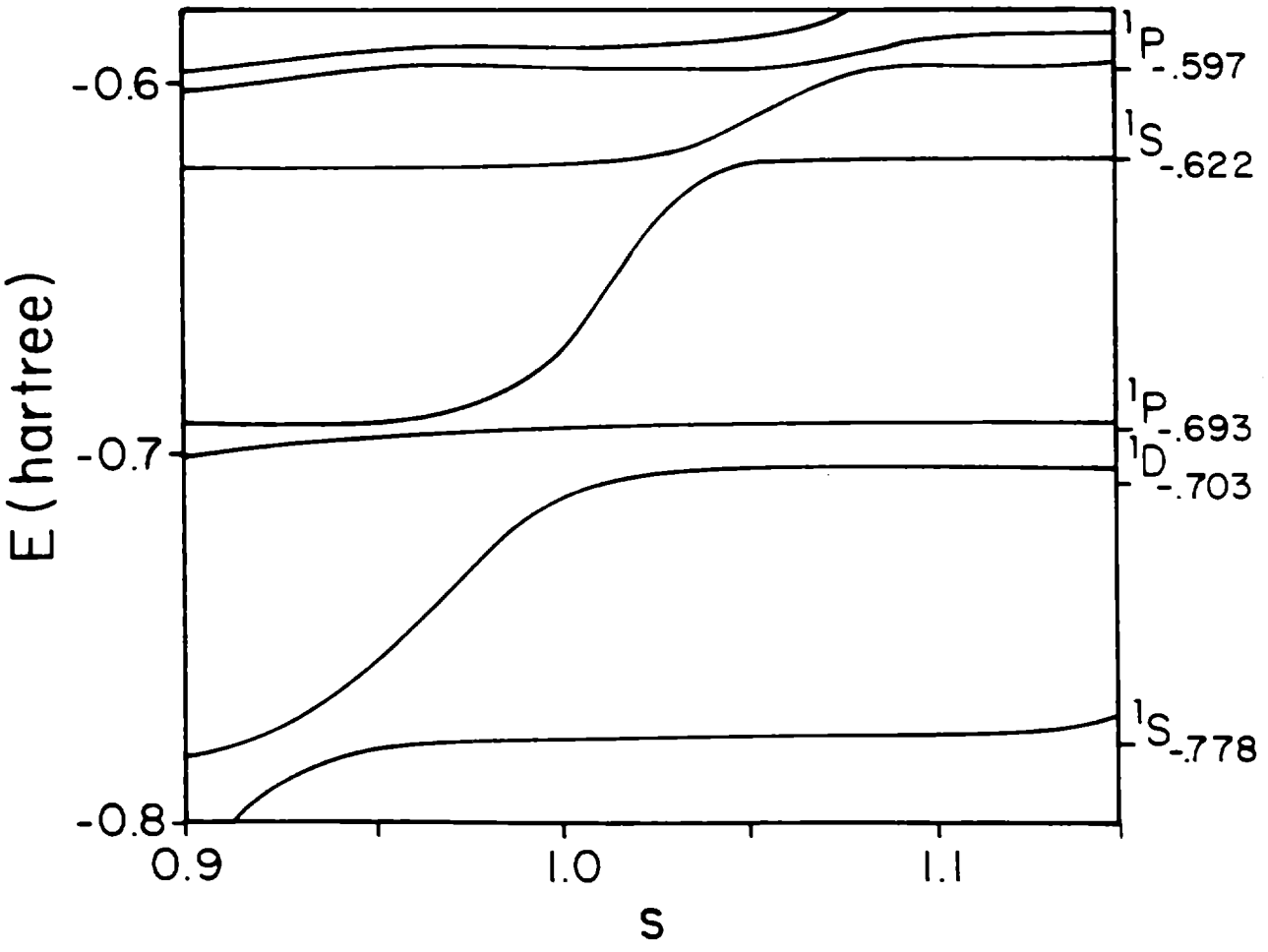

FIGURE 5

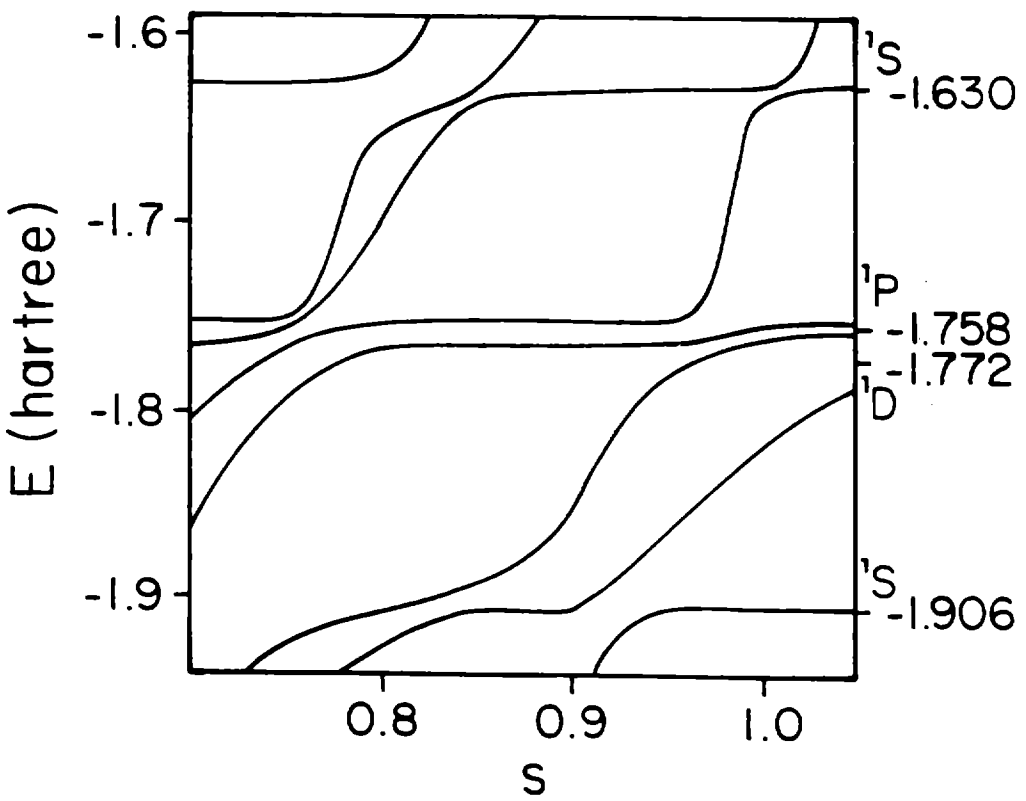

FIGURE 6

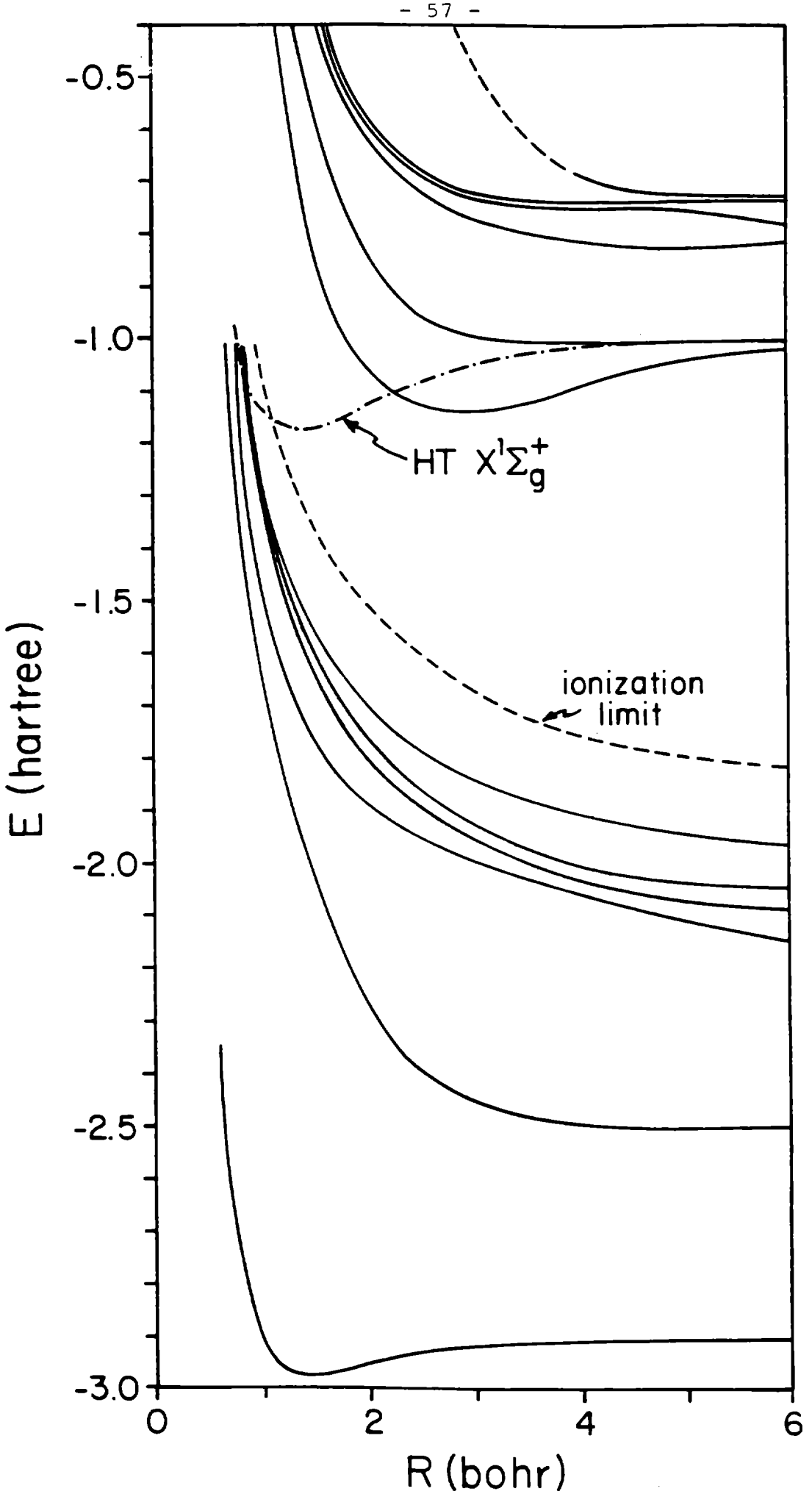
-0.5
-1.0
-1.5
-2.0
-2.5
-3.0
E (hartree)
HT $X^1\Sigma_g^+$
ionization
limit
0
2
4
6
R (bohr)

FIGURE 7